Available online at www.sciencedirect.com
SCIENCE DIRECT®
European Polymer Journal 41 (2005) 447–452
EUROPEAN POLYMER JOURNAL
www.elsevier.com/locate/europolj

Light scattering studies of stereocomplex formation of stereoregular poly(methyl methacrylate) in solutions

Yue Zhao [a,b,*], Wenna Chen [a], Dennis Hair [a], Jian Xu [a], Chi Wu [b,c], Charles C. Han [a]

[a] State Key Laboratory of Polymer Physics and Chemistry, Institute of Chemistry, Chinese Academy of Science, Beijing 100080, PR China
[b] The Open Laboratory of Bond-selective Chemistry, Department of Chemical Physics, University of Science and Technology of China, Hefei, Anhui 230026, PR China
[c] Department of Chemistry, The Chinese University of Hong Kong, Shatin, N.T., Hong Kong

Received 20 August 2004; accepted 21 October 2004
Available online 24 December 2004

Abstract

The structure and stereocomplex formation of multi-stereoblock poly(methyl methacrylates) in three different solvents, acetone, tetrahydrofuran (THF) and chloroform, corresponding to strongly-, weakly- and non-complexing solvent, respectively, were investigated by a combination of static and dynamic laser light scattering. Our results revealed that the stereocomplex was caused by weak interactions, and could be melted at higher temperatures. In THF, the intermolecular and intramolecular interactions could be clearly separated at lower temperatures, and the structure of aggregated chains was linear. In acetone, a more compact structure was obtained, which was corroborated by the fact that the stereocomplex had a higher melting temperature than in THF.

Keywords: Poly(methyl methacrylate); Stereocomplex; Laser light scattering

1. Introduction

Stereocomplex formation between isotactic and syndiotactic poly(methyl methacrylates) (PMMA) has been investigated since 1958 [1]. Most of this work has been reviewed by Spevacek et al. and te Nijenhuis et al. [2,3]. Stereocomplex formation depends on stereoregularity [4], mixing ratio [5–8] and concentration of tactic polymers [5,9,10], as well as on the temperature [11–14], and most of all, the solvent type [15–18]. Solvents can be classified according to their tendency to stimulate the stereocomplex formation: strongly complexing solvents (e.g., dimethylformamide (DMF), acetonitrile, tetrachloromethane, acetone); weakly complexing solvents (e.g., toluene, benzene); and non-complexing solvents (e.g., chloroform, dichloromethane) [11,12]. It is known that the stereocomplex of stereoregular PMMA chains form helical structures in solution, which exist naturally, especially occurring in biopolymers, such as proteins,

* Corresponding author. Present address: Department of Polymer Chemistry, Kyoto University, Kyoto 615-8510, Japan. Tel.: +81 753 832 619; fax: +81 753 832 623.
E-mail address: yzhao@alloy.polym.kyoto-u.ac.jp (Y. Zhao).

0014-3057/$ - see front matter © 2004 Elsevier Ltd. All rights reserved.
doi:10.1016/j.eurpolymj.2004.10.031

Table 1
Characteristics of poly(methyl methacrylate) from gel permeation chromatography (GPC) at $T = 40$ °C in THF, and ^{1}H NMR spectrum

Samples	M_n/(g/mol)	M_w/M_n	Triad distribution mm/rr/mr	Average degree of polymerization (monomer units)
PMMA-1	3.19×10^4	1.25	40.3/37.1/22.6	5
PMMA-2	3.29×10^4	1.24	37.0/38.7/24.3	4

polysaccharides and DNA [19–21]. Because of this, stereocomplex formation between PMMA chains may be applied to study the polymeric assembly from solution as a model system. The stereocomplex formation of uniform stereoblock PMMA especially attracted attention, for an intramolecular complexation and an intermolecular complexation are both obtained [6,7].

Among the studies of stereocomplex formation of PMMA, various physical and physico-chemical methods have been used, including dilute solution methods (turbidimetry [11,18,22], classical light scattering [23–25], spin label methods [26,27], gel permeation chromatography (GPC) [6,7,24], and viscometry [28,29], etc.), methods for concentrated solution and gels (differential scanning calorimetry (DSC) [11,30], X-ray diffraction [31], etc.), and molecular spectroscopic methods (NMR spectroscopy [32], IR and Raman spectroscopy [30]). It has been convinced that the complexation was caused by weak interaction, with their results enhanced by cooperative effects. The stoichiometries reported in the past concern the ration of the weight fractions of it- and st-PMMAs. Stereocomplex forms between the stoichiometries it/st = 1.5 and 0.5, and the melting point of the complex decreases with the decreasing tacticity of the st-component. There exists a minimum chain-length required for the stereocomplex formation, which varies with solvent [2]. However, the structure of the complex formation is still ambiguous, and data evidence for complexation in solution is still less.

In this paper, a combination of dynamic light scattering and static (classical) light scattering is used for the first time to study the stereocomplex formation of PMMA in solution. Three solvents, acetone, tetrahydrofuran (THF) and chloroform, corresponding to strongly, weakly and non-complexing solvents, respectively, were used to study the stereocomplex formation of stereoblock PMMAs. The present work may give a better understanding of the relationship between polymer structure and properties.

2. Experimental

2.1. Sample preparation

Multi-stereoblock poly(methyl methacrylates) were offered by Prof. Eugene Y. Chen of Colorado State University. The details of the synthesis can be found elsewhere [33]. Both samples have relatively narrow molecular weight distributions and high stereoregularity of both isotactic and syndiotactic blocks. GPC and ^{1}H NMR results for the two samples are listed in Table 1.

All the samples are dissolved to a desired concentration. Before LLS measurement, the solution was kept at −23 °C for 24 h, then aged at the desired temperatures until no change.

2.2. Laser light scattering (LLS)

A commercial LLS spectrometer (ALV/SP-125) equipped with a multi-tau digital time correlator (ALV-5000) and a He–Ne laser (JDS Uniphase corporation, model 1145p-3083, output power = ~35 MW at $\lambda = 632.8$ nm) was used. In static LLS, the angular dependence of the excess absolute time-average scattered intensity, i.e. Rayleigh ratio $R_{vv}(q)$, of a dilute dispersion leads to the weight-average molar mass M_w, the second virial coefficient A_2 and the root-mean square z-average radius of gyration $\langle R_g^2 \rangle_z^{1/2}$ (or simply as $\langle R_g \rangle$), where q is the scattering vector, equals to $q = \frac{4\pi n \sin(\frac{\theta}{2})}{\lambda}$, where n is the reflective index of the solvent, θ is the scattering angle and λ is the wave length of the light. In dynamic light scattering (DLS), the cumulant analysis of the measured intensity–intensity time correlation function $G^{(2)}(q,t)$ in the self-beating mode provides an average line-width ($\langle \Gamma \rangle$), and Laplace inversion analysis provides the line-width distribution ($G(\Gamma)$) [34,35]. For a pure diffusive relaxation, Γ can be related to the translational diffusion coefficient D via $\Gamma = Dq^2$ in the limit of $c \to 0$ and $q \to 0$ [34], where c is the concentration of scatters. The hydrodynamic radius (R_h) can be calculated by the Stokes-Einstein equation $D = k_B T/(6\pi\eta R_h)$. where k_B is the Boltzmann constant, T is the absolute temperature, and η is the solvent viscosity. Therefore, $G(\Gamma)$ can be converted to a hydrodynamic radius distribution $f(R_h)$: From each line width distribution $G(\Gamma)$ or hydrodynamic radius distribution $f(R_h)$, we calculate an average line width ($\langle \Gamma \rangle$, defined as $\int_0^\infty G(\Gamma)\Gamma \mathrm{d}\Gamma$) or an average hydrodynamic radius ($\langle R_h \rangle$, defined as $\int_0^\infty f(R_h)R_h \mathrm{d}R_h$) characteristic of the sample. Polydispersity Index (PDI) is calculated from the second moment ($\mu_2 = \int_0^\infty (\Gamma - \overline{\Gamma})^2 G(\Gamma)\,\mathrm{d}\Gamma$), was PD.I. $= \frac{\mu_2}{\overline{\Gamma}^2}$.

The PMMA solutions were clarified by 0.45 μm Millipore Nylon filters to remove dust. $R_{vv}(q)$ and $G^{(2)}(t,q)$ were simultaneously measured during the experiments.

The detail of the LLS instrumentation can be found elsewhere [36].

3. Results and discussion

Fig. 1(a) and (b) show the temperature dependence of the average hydrodynamic radius ($\langle R_h \rangle$), and weight average molar mass ($\langle M_w \rangle$) in THF, respectively. Both $\langle R_h \rangle$ and $\langle M_w \rangle$ of the PMMAs decrease with the increasing temperature, until ~28 °C, at which they are unchanging. It indicates that the intermolecular stereocomplex is formed at lower temperatures and decomposed at higher temperatures, which is consistent with the results given in Ref. [6,7]. The complex formation of PMMA-1 is more pronounced than PMMA-2, which is reasonable due to the higher stereoregularity. It should be noted that both the size and molar mass changed rapidly with temperature, which reveals that the intermolecular stereocomplex is caused by weak interactions and sensitive to temperatures.

Fig. 2 shows typical decay time (τ) distributions of PMMA-1 in THF at different temperatures in heating process. It is interesting to see that the decomposition of the stereo-complex can be divided into three temperature regimes. First, at low temperatures, there are two peaks, one is attributed to the intramolecular complex, which appears as a fast mode. The other one is attributed to both the intermolecular complex and non-complexed single chains, which appears as a slow mode. These two peaks are clearly separated in the first regime. In the second regime, as the temperature increases, the two separated peaks merged into a single narrowly distributed peak. This regime is before the single chain stage, because a relatively slower motion than the final state is observed. Note that the decay time is proportional to the average hydrodynamic radius from Stocks–Einstein equation $\tau = \frac{6\pi\eta R_h}{kTq^2}$. In the third temperature regime, which is higher than 32 °C, neither intra- nor intermolecular stereocomplex can be seen, and the scattering is completely due to the single chains, which results in a little broader peak because of the polydispersity of the single chains. The inset shows the temperature dependence of the polydispersity index (PDI). It shows a decreasing tendency at first, until reaching the temperature around 32 °C, then a little increase with temperature. It is noted that in the second regime, the small fast peak due to the intramolecular complex disappeared altogether. However, the slower mode appeared to be caused by intermolecular complexation, corresponding to the low PD. I. This result is an additional evidence for the three stages scheme we discussed above.

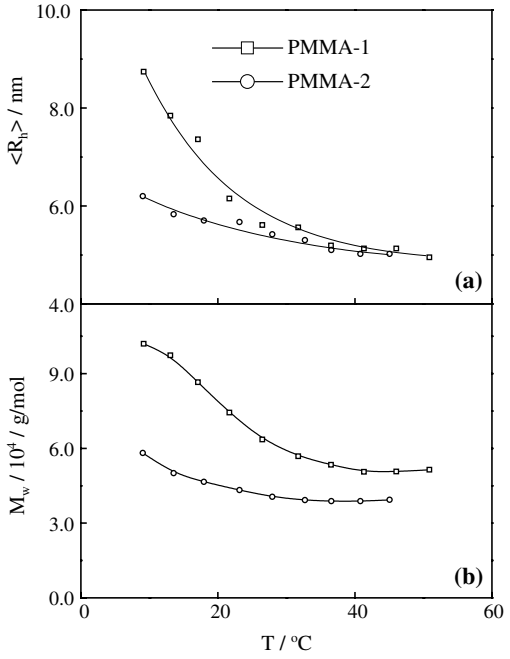

Fig. 1. Temperature dependence of the average hydrodynamic radii and the weight average molar mass of PMMAs in THF, where $C_{PMMAs} = 4.29 \times 10^{-3}$ g/ml.

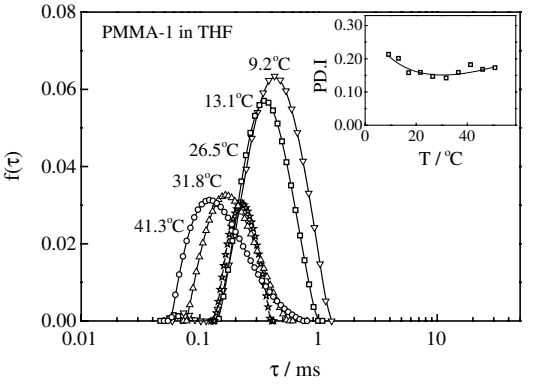

Fig. 2. Temperature dependence of the hydrodynamic radius distributions of PMMA-1 in THF, where $C_{PMMA-1} = 4.29 \times 10^{-3}$ g/ml and $\theta = 15°$. The inset is temperature dependence of the polydispersity index of PMMA-1 in THF.

The dynamics of the disassembly of PMMA-1 complexation at $T = 40$ °C is shown in Fig. 3. The complex was formed as described in the sample preparation section and light scattering measurements was carried out when temperature was stable. Both the size and the molecular weight of the PMMA complex decrease with time as power law function. Note that at small angle, the scattering intensity (I) is proportional to the molecular weight of the complex. The scaling between $\langle R_h \rangle$ or I and t follows $\langle R_h \rangle \sim t^{-0.081\pm0.001}$, $I \sim t^{-0.063\pm0.001}$. We plot the decrease of I against the corresponding average hydrodynamic radius $\langle R_h \rangle$ in Fig. 4 and get

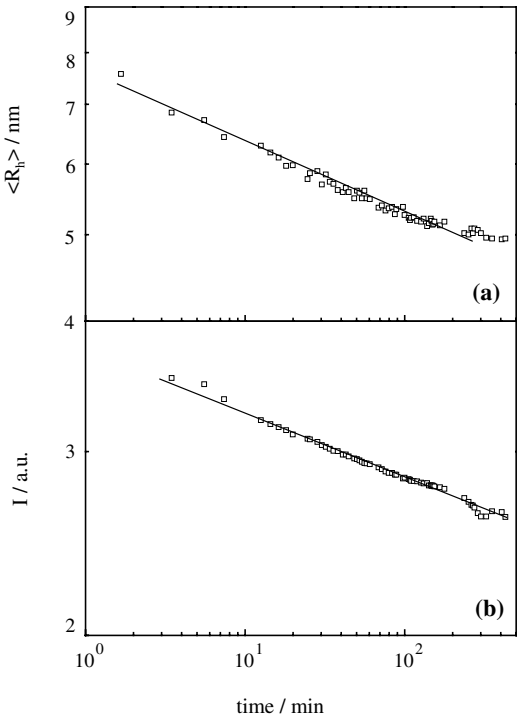

Fig. 3. Time dependence of the average hydrodynamic radii and the scattering intensity of PMMA-1 in THF, where $C_{PMMA-1} = 4.29 \times 10^{-3}$ g/ml and $T = 40$ °C.

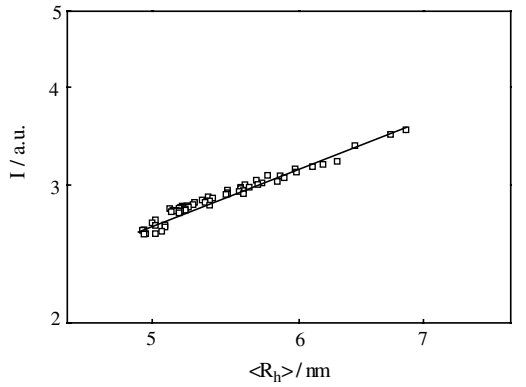

Fig. 4. Scaling of the scattering intensity and the average hydrodynamic radius of PMMA-1, where $C_{PMMA-1} = 4.29 \times 10^{-3}$ g/ml and $T = 40$ °C.

$I \sim \langle R_h \rangle^{0.88\pm0.02}$, indicating that these PMMA-1 chains stick to each other in a linear fashion.

Fig. 5a and b show that the average hydrodynamic radius and the weight average molar mass of the PMMA samples decrease with increasing temperature in acetone. Both the average hydrodynamic radius and the average aggregation number (N_{agg}) in each complex, which is calculated from $N_{agg} = \frac{M_{w,aggregate}}{M_{w,chain}}$, become much

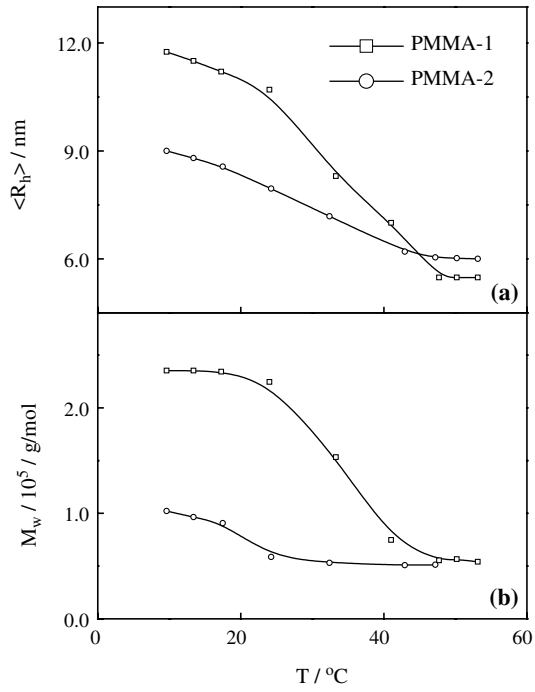

Fig. 5. Temperature dependence of the average hydrodynamic radii and the weight average molar mass of PMMAs in acetone, where $C_{PMMAs} = 2.88 \times 10^{-3}$ g/ml.

larger than that of in THF. It also clearly shows that the melting of such formed stereocomplex becomes more difficult, and the completely melting temperature rises to 47 °C. It should be noted that in acetone, the intermolecular complex is much stronger, which has overlapped the information from the intramolecular complex.

In Fig. 6, we plot the increase of M_w against the corresponding average hydrodynamic radius of PMMA-1

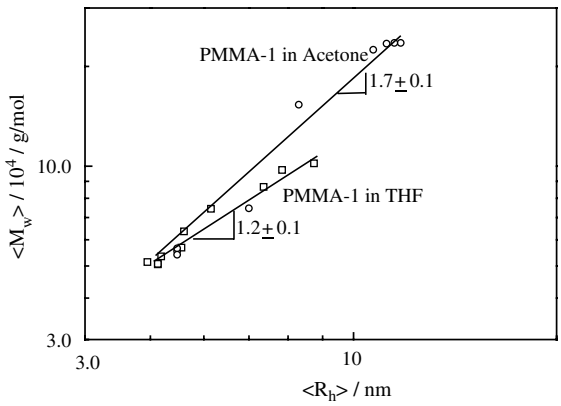

Fig. 6. Scaling relationships between the weight average molar mass and the hydrodynamic radius of PMMA-1 in THF and acetone.

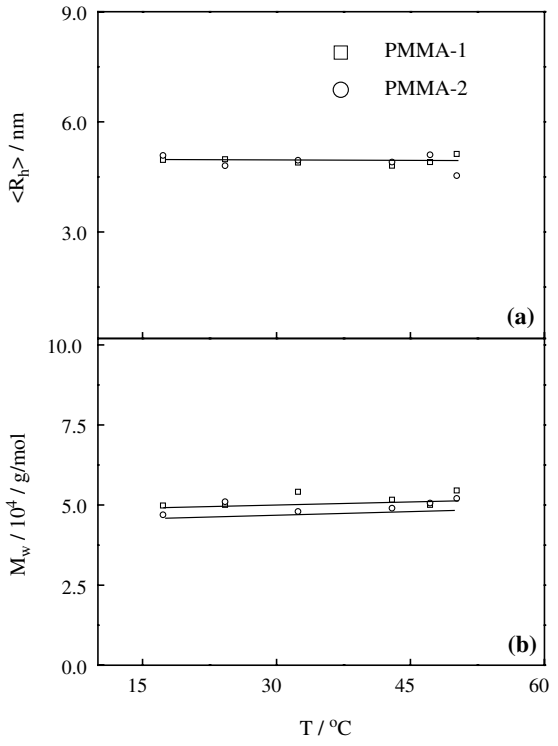

Fig. 7. Temperature dependence of the average hydrodynamic radii and the weight average molar mass of PMMAs in chloroform, where $C_{PMMAs} = 2.80 \times 10^{-3}$ g/ml.

in THF and acetone at different temperatures. In THF, $M_w \sim \langle R_h \rangle^{1.2\pm0.1}$, showing that each aggregate, on average, contains only a few chains, and these chains are connected in a linear fashion, consistent with the helical structure reported in the literature. In acetone, $M_w \sim \langle R_h \rangle^{1.7\pm0.1}$. The fractal exponents in both solvents are larger than 1. This indicates the resultant stereocomplex has a rod-like fashion, where the cross section can not be neglected comparing with the rod length. The fractal exponent is much higher in acetone, reflecting a more compact structure of the complexes.

Fig. 7a and b show the temperature dependence of PMMA in chloroform. These data clearly show that no complex was formed even at lower temperatures, which is consistent with chloroform being a non-complexing solvent for stereoblock PMMAs. The lack of temperature dependence makes chloroform an excellent eluent for sample calibration in GPC.

4. Conclusions

Novel synthetic multistereoblock poly(methyl methacrylates) are studied in three different solvents: acetone, THF and chloroform, which corresponding to strongly, weakly and non-complexing solvents, respectively. A combination of dynamic and static (classical) light scattering is used for the first time to follow the stereocomplex formation in these solvents. Our results show that the stereocomplex is caused by weak interactions, and can be melted at higher temperatures. Compared with acetone, THF is a particularly weakly complexing solvent. In THF, the complex has a melting temperature at 32 °C. The intermolecular and intramolecular interaction can be clearly separated at lower temperatures. There are three stages in the melting process. Firstly, two peaks appear clearly at lower temperatures; secondly, the faster mode peak disappears, leaving one narrow peak, due to the intermolecular complex; and finally, the intermolecular aggregates melt into single chains, resulting in a broad peak. Acetone is a stronger complexing solvent than THF, and the melting temperature of the complex moves to a higher temperature of 47 °C. The stereocomplex formed in acetone is more compact.

Acknowledgements

The financial support of the CAS Bai Ren Project, the NSFC projector (29974027) and the HKSAR Earmarked RGC Grants (CUHK4266/00P, 2160135) is gratefully acknowledged.

References

[1] Fox TG, Carrett BS, Goode WE, Gratch S, Kincaid JF, Spell A, et al. J Am Chem Soc 1958;80:1768.
[2] Spevacek J, Schneider B. Adv Colloid Interface Sci 1987;27:81.
[3] te Nijenhuis K. Adv Polym Sci 1997;130:67.
[4] Dybal J, Spevacek J, Schneider B. J Polym Sci, Polym Phys Ed 1986;24:657.
[5] Hamada K, Serizawa T, Kitayama T, Fujimoto N, Hatada K, Akashi M. Langmuir 2001;17:5513.
[6] Hatada K, Kitayama T, Ute K, Nishiura T. Macromol Symp 1998;132:221.
[7] Hatada K. J Polym Sci, Polym Chem Ed 1999;37:245.
[8] Mizumoto T, Sugimura N, Moritani M, Sato Y, Masuoka H. Macromolecules 2001;34:1291.
[9] Grohens Y, Castelein G, Carriere P, Spevacek J, Schultz J. Langmuir 2001;17:86.
[10] Serizawa T, Hamada K, Kitayama T, Fujimoto N, Hatada K, Akashi M. J Am Chem Soc 2000;122:1891.
[11] Lemieux EJ, Prud'homme RE. Polymer 1998;39:5453.
[12] Fazir N, Brulet A, Guenet JM. Macromolecules 1994;27:3836.
[13] Watanabe WH, Ryan CF, Fleischer PC, Garrett BS. J Phys Chem 1961;65:896.
[14] Liquori AM, Anzuino G, Coiro VM, D'Alagni M, De Santis P, Savino M. Nature 1965;206:358.
[15] Challa G, de Boer A, Tan YY. Int J Polym Mater 1976;4:239.

[16] Vorenkamp EJ, Bosscher F, Challa G. Polymer 1979;20:59.
[17] Katime I, Quintana JR, Veguillas J. Polymer 1983;24:903.
[18] Bistac S, Schultz J. Macromol Chem Phys 1997;198:531.
[19] Bosscher F, Brinke GT, Challa G. Macromolecules 1982;15:1442.
[20] Spevacek J. Macromol Chem, Macromol Symp 1990;39:71.
[21] Schomaker E, Challa G. Macromolecules 1989;22:3337.
[22] Buter R, Tan YY, Challa G. J Polym Sci Polym Chem Ed 1973;11:2975.
[23] Chiang R, Burke JJ, Threlkeld JO, Orofino TA. J Phys Chem 1966;70:3591.
[24] Vorenkamp EJ, Challa G. Polymer 1981;22:1705.
[25] Nakamura Y, Nakagawa T, Sasaki N, Yamagishi A, Nakata M. Macromolecules 2001;34:5984.
[26] Ito T, Ohnishi S. Rep Prof Polym Phys Japan 1972;15:477.
[27] Morawetz H, Fernandez-Pierola I, Jachowicz J, Chen HL. Polym Prepr 1982;23:12.
[28] Rehage G, Wagner D. Polym Prepr 1982;23:29.
[29] Quadrat O, Belnikevitch NG. Polymer 1983;24:719.
[30] Wang JJ, Zhao J, Gu Q, Shen DY. Macromol Rapid Commun 2001;22:948.
[31] de Boer A, Challa G. Polymer 1976;17:633.
[32] Spevacek J, Schneider B, Straka J. Macromolecules 1990;23:3042.
[33] Chen EYX, Cooney MJ. J Am Chem Soc 2003;125:7150.
[34] Chu B. Laser light scattering. second ed. New York: Academic Press; 1991.
[35] Berne B, Pecora R. Dynamic light scattering. New York: Plenum Press; 1976.
[36] Wu C, Zhou SQ. Macromolecules 1995;28:8381.